

ChemComm

Accepted Manuscript



This is an *Accepted Manuscript*, which has been through the Royal Society of Chemistry peer review process and has been accepted for publication.

Accepted Manuscripts are published online shortly after acceptance, before technical editing, formatting and proof reading. Using this free service, authors can make their results available to the community, in citable form, before we publish the edited article. We will replace this *Accepted Manuscript* with the edited and formatted *Advance Article* as soon as it is available.

You can find more information about *Accepted Manuscripts* in the [Information for Authors](#).

Please note that technical editing may introduce minor changes to the text and/or graphics, which may alter content. The journal's standard [Terms & Conditions](#) and the [Ethical guidelines](#) still apply. In no event shall the Royal Society of Chemistry be held responsible for any errors or omissions in this *Accepted Manuscript* or any consequences arising from the use of any information it contains.



Journal Name

COMMUNICATION

Amine Grafted Silica Supported CrAuPd Alloy Nanoparticles: A Superb Heterogeneous Catalyst for the Room Temperature Dehydrogenation of Formic Acid[†]

Received 00th January 20xx,
Accepted 00th January 20xx

DOI: 10.1039/x0xx00000x

www.rsc.org/

Mehmet Yurderi,^a Ahmet Bulut,^a Nurdan Caner,^a Metin Celebi,^a Murat Kaya^b and Mehmet Zahmakiran^{a,*}

Herein we show that a previously unappreciated combination of CrAuPd alloy nanoparticles and amine-grafted silica support facilitates the liberation of CO-free H₂ from dehydrogenation of formic acid with record activity in the absence of any additives at room temperature. Furthermore, their excellent catalytic stability make them isolable and reusable heterogeneous catalyst in the formic acid dehydrogenation.

Hydrogen (H₂) is considered to be a promising energy carrier for our future society as it is light-weight and has a high energy density (142 MJ/kg), almost three times higher than that of natural gas (55 MJ/kg).¹ In addition to possessing light weight and high energy density, hydrogen is also an environmentally friendly energy vector to end users when combined with proton exchange membrane fuel cells (PEMFC), since only water and small amounts of heat are the by-products when it is utilized in PEMFC.² However, controlled storage and release of hydrogen are still technological barriers in the fuel cell based hydrogen economy.^{1,2} In this context, formic acid (FA, HCOOH), which is one of the major stable and non-toxic liquid products formed in biomass processing, has attracted recent attention as a suitable hydrogen carrier for fuel cells designed for portable use.³ In the presence of metal catalysts, FA can catalytically be decomposed via dehydrogenation (HCOOH → H₂ + CO₂) and dehydration (HCOOH → H₂O + CO) pathways.³ The selective dehydrogenation of FA is indispensable for the production of ultrapure H₂, since toxic carbon monoxide (CO) produced by dehydration pathway significantly reduces the activity of Pt catalyst in PEMFC.⁴ Recently, serious efforts have been done in the development of homogeneous catalysts for the selective dehydrogenation of FA.⁵ Even though, the notable activities have been reported by some of these,⁶ the difficulties met during their isolation-recovery steps hinder their practical application for on-board systems. At this concern, the current research has been focused on the development of practical heterogeneous catalysts^{7,8}

that exhibit significant activity under mild conditions with painless synthesis and recovery routes. In spite of the tremendous labour, the majority of the reported heterogeneous catalysts for FA dehydrogenation needs extra additives (e.g. HCOONa, LiBF₄ etc.) and elevated temperatures.⁷ Until now, only a few heterogeneous catalysts⁸ have been found to provide notable activities in the additive-free FA dehydrogenation at low temperatures. In this regard, the development of highly active, selective and reusable solid catalysts that operates at low temperatures for FA dehydrogenation in the absence of additives is of great importance. Herein, we present a facile synthesis of CrAuPd alloy nanoparticles (NPs) supported on 3-aminopropyltriethoxysilane functionalized silica, hereafter referred to as CrAuPd/N-SiO₂, and their excellent catalysis in the additive-free dehydrogenation of FA at room temperature.

CrAuPd/N-SiO₂ can reproducibly be prepared through a simple impregnation route followed by subsequent sodium borohydride (NaBH₄) reduction in water all at room temperature.⁹ After centrifugation, copious washing with water, CrAuPd/N-SiO₂ were isolated as gray powders and characterized by multi-pronged techniques. The molar composition of the as-prepared catalyst was found to be Cr_{0.15}Au_{0.40}Pd_{0.60} (0.21 % wt Cr, 1.26 % wt Au and 1.65 % wt Pd loadings correspond to 4.0 μmol Cr, 6.6 μmol Au and 16.0 μmol Pd, 0.98 mmol NH₂/g SiO₂) by inductively coupled plasma-optical emission spectroscopy (ICP-OES) and ninhydrin method. The conventional transmission electron microscopy (CTEM), high resolution-TEM (HRTEM), scanning TEM-energy dispersive X-ray spectroscopy (STEM-EDX) and high angle annular dark field scanning transmission electron microscopy (HAADF-STEM) investigations were performed to examine the size, morphology and the composition of the CrAuPd/N-SiO₂ catalyst. CTEM images of CrAuPd/N-SiO₂ given in Figs. 1(a) and b reveal the presence of CrAuPd NPs. The mean particle size for the images given in Figs. 1(a) and (b) was found to be ca. 2.6 nm by the particle size analysis of > 100 non-touching particles (Fig. 1(a) inset). STEM-EDX analysis of large number of different domains on the CrAuPd/N-SiO₂ surface revealed that the presence of Cr, Au, and Pd in the analyzed region (Fig. 1(b) inset). HRTEM image of CrAuPd/N-SiO₂ is given in Fig. 1(c) displays the highly crystalline nature of the NPs on the N-SiO₂.

^aDepartment of Chemistry, Science Faculty, Yuzuncu Yil University, 65080, Van, Turkey. E-mail: zmehmet@yyu.edu.tr; Web: www.nanomatcat.com

^bDepartment of Chemical Engineering and Applied Chemistry, Atilim University, 06836, Ankara, Turkey.

[†] Electronic Supplementary Information (ESI) available: [Detailed synthesis protocols, experimental procedures, activity results, TEM, FTIR, XPS, GC characterization]. See DOI: 10.1039/x0xx00000x

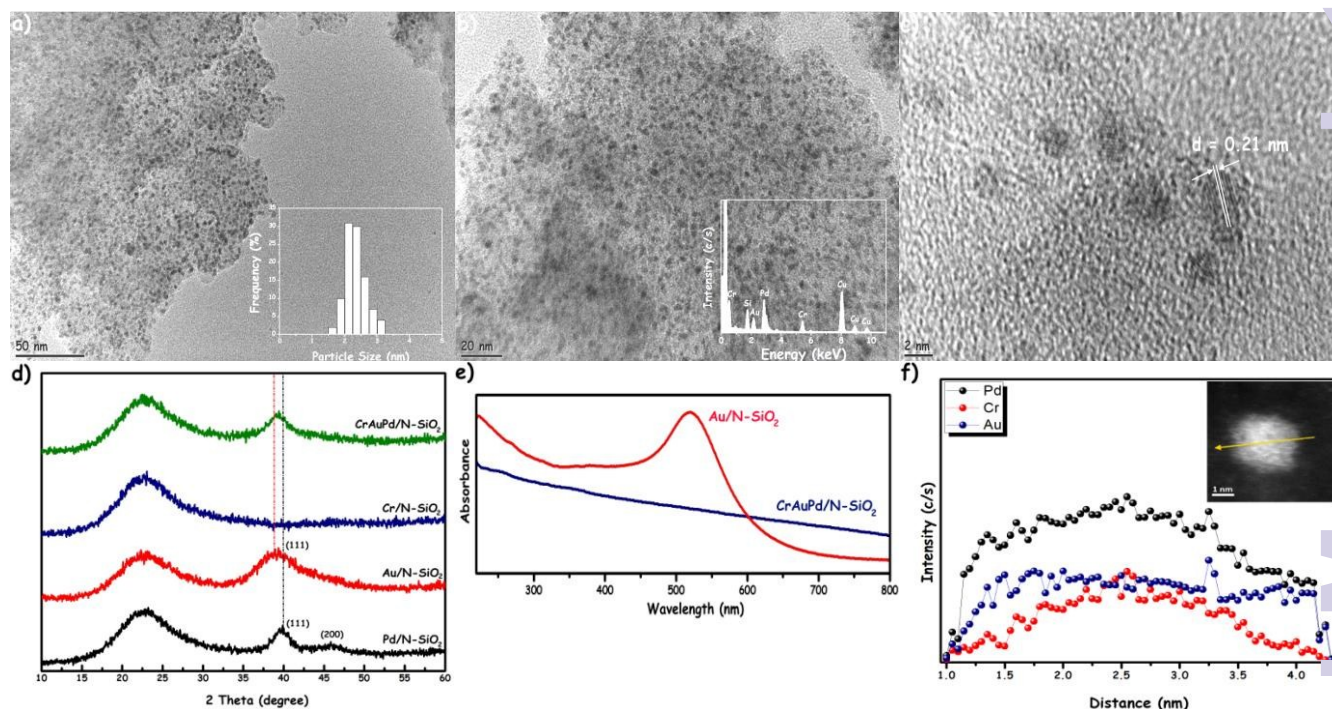


Fig. 1. (a) CTEM image and corresponding size histogram, (b) CTEM and TEM-EDX spectrum, (c) HRTEM image of CrAuPd/N-SiO₂, (d) P-XRD patterns of CrAuPd/N-SiO₂, Cr/N-SiO₂, Au/N-SiO₂, Pd/N-SiO₂, (e) DR-UV-vis spectra of CrAuPd/N-SiO₂ and Au/N-SiO₂, (f) HAADF-STEM image and line scan analysis spectrum of CrAuPd/N-SiO₂.

The crystalline fringe distance was measured to be 0.21 nm, which is different from (111) spacing of the face-centered cubic (fcc) Au (0.235 nm),^{8(e)} Pd (0.223 nm)^{8(e)} and (110) spacing of Cr (0.263 nm).¹¹ In addition to that, the powder X-ray diffraction (P-XRD) pattern of the as-synthesized catalyst (Fig. 1(d)) exhibits a diffraction peak in the position between Pd (111) and Au (111), whose position also differs from Cr (110).¹¹ Diffuse reflectance UV-Vis (DR-UV-Vis) spectrum taken from solid powders of CrAuPd/N-SiO₂ (Fig. 1(e)) show almost no surface plasmon resonance band for Au NPs, whereas Au/N-SiO₂ have surface plasmon resonance bands at near 440 nm. This surface plasmon resonance quenching caused by alloying was also observed in PdAu^{8(e)} and PdAg^{8(f)} alloy NPs. Furthermore, the formation of alloy structure was also confirmed by HAADF-STEM-line analysis (Fig. 1(f)). When the distribution of Cr, Au and Pd in the randomly chosen particle was assessed by using the line scanning analysis in the STEM-EDX mode, we can clearly see the overlapping of Cr, Au and Pd signals that can be assignable to the formation of alloy structure in CrAuPd NPs. Additionally, X-ray photoelectron spectroscopy (XPS) results reveal that the binding energies for Pd 3d and Au 4f in CrAuPd/N-SiO₂ are shifted to the lower values with respect to those in Pd/N-SiO₂ and Au/N-SiO₂, respectively; whereas Cr 2p binding energy is shifted to higher value compared with that of Cr/N-SiO₂ (Fig. S1, ESI[†]). These shifts are indicative of transferring of some electrons from Cr to Pd and Au to equalize Fermi level owing to the difference of work functions of Pd (5.67 eV), Au (5.54 eV) and Cr (4.5 eV). This electron transfer in CrAuPd/N-SiO₂ has the potential design itself with the high activity in FA dehydrogenation (*vide infra*) as the increase in the electron density of catalytically active Pd and Au centers facilitates metal-formate formation in the FA decomposition, which enhances the rate of the catalytic dehydrogenation of FA.¹²

The catalytic activities of Cr_{0.15}Au_{0.40}Pd_{0.60}/N-SiO₂ together with its monometallic, bimetallic and trimetallic counterparts in different molar compositions were investigated in the dehydrogenation of aqueous FA solution (0.20 M in 10.0 mL H₂O) at 298 K and their results are given in Figs 2 (a)-(c). Evidently, Cr_{0.15}Au_{0.40}Pd_{0.60}/N-SiO₂ catalyst provides a better activity than those of mono and bimetallic catalysts prepared by the same method. From Figs. 2 (a) and (b), it is clear that Pd is the crucial active metal in all catalysts; without Pd addition Cr_{1.0}/N-SiO₂, Au_{1.0}/N-SiO₂, and Cr_{0.49}Au_{0.51}/N-SiO₂ catalysts show almost no activity. On the other hand, the initial activity of monometallic Pd (Pd_{1.0}/N-SiO₂) cannot resume as the active sites are easily deactivated by poisonous CO intermediate, which is one of important obstacles for the application monometallic catalysts in FA dehydrogenation.³ Although, bimetallic Cr_{0.48}Pd_{0.52}/N-SiO₂ and Au_{0.45}Pd_{0.55}/N-SiO₂ catalysts show better activities than Pd_{1.0}/N-SiO₂, their performances are still far inferior to the trimetallic Cr_{0.15}Au_{0.40}Pd_{0.60}/N-SiO₂. The morphological investigation by CTEM analyses (Fig. S2, ESI[†]) reveals that mono and bimetallic catalysts have similar shapes and sizes with respect to Cr_{0.15}Au_{0.40}Pd_{0.60}/N-SiO₂. The enhanced catalytic activity of Cr_{0.15}Au_{0.40}Pd_{0.60}/N-SiO₂ may be attributed to its special composition and surface electronic state in the formed alloy structure,¹³ which was further supported by the result of a control experiment in which the physical mixture of Cr_{0.17}/N-SiO₂, Au_{0.23}/N-SiO₂ and Pd_{0.60}/N-SiO₂ exhibits lower activity than Cr_{0.15}Au_{0.40}Pd_{0.60}/N-SiO₂ catalyst in FA dehydrogenation under identical conditions (Fig. S3, ESI[†]). The generated gas obtained during Cr_{0.15}Au_{0.40}Pd_{0.60}/N-SiO₂ catalyzed FA dehydrogenation was analyzed by gas chromatography (GC), infrared spectroscopy (FTIR) and NaOH trap experiment (Figs. S3-S6, ESI[†]). Their results revealed that the generated gas is a mixture of H₂ and CO₂ with a H₂:CO₂ molar ratio of 1.0:1.0 where CO was below the detection limit (*i.e.* <

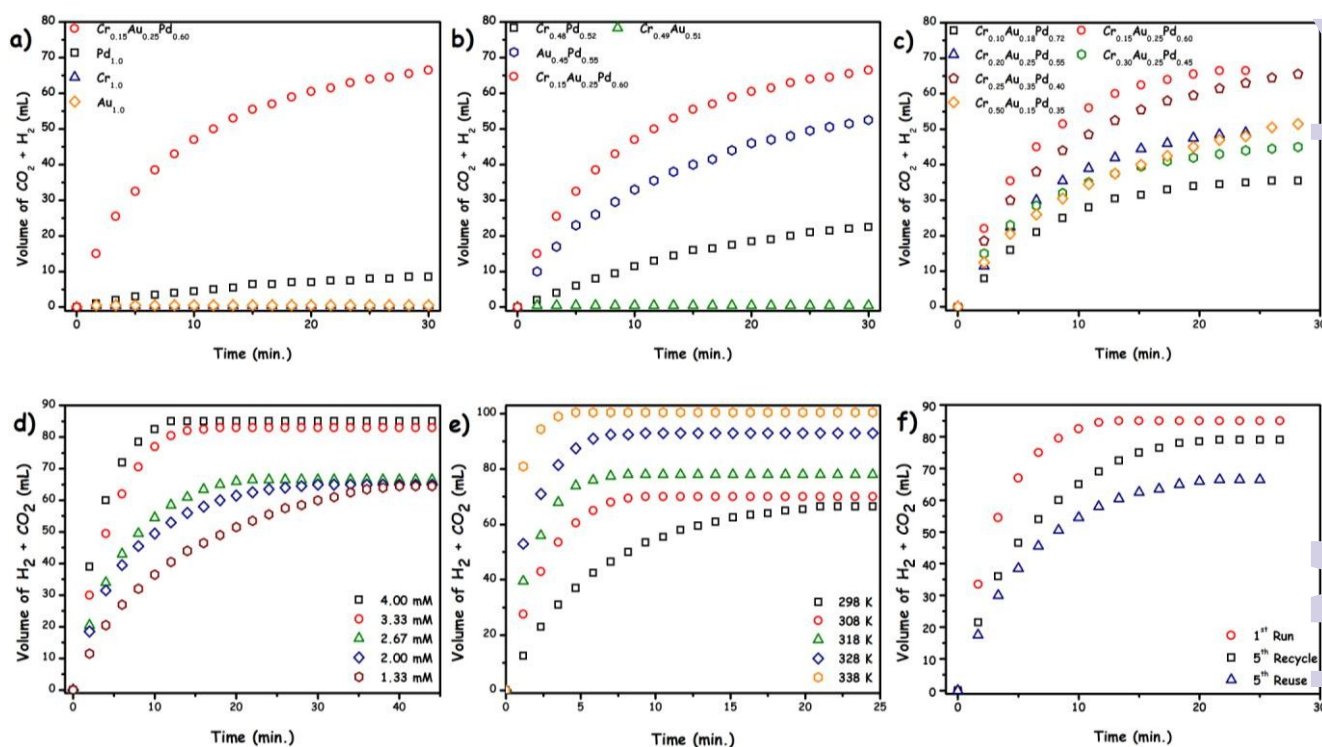


Fig. 2. The volume of gas ($\text{CO}_2 + \text{H}_2$) (mL) versus time (min.) graphs for the catalytic dehydrogenation of aqueous FA solution (0.20 M in 10.0 mL H_2O) catalyzed by (a) monometallic, (b) bimetallic, (c) trimetallic catalysts (in all [catalyst] = 2.67 mM), (d) $\text{Cr}_{0.15}\text{Au}_{0.25}\text{Pd}_{0.60}/\text{N-SiO}_2$ catalyst at different [CrAuPd] concentrations at 298 K, (e) $\text{Cr}_{0.15}\text{Au}_{0.25}\text{Pd}_{0.60}/\text{N-SiO}_2$ catalyst at different temperatures, and (f) reusability and recyclability performances of $\text{Cr}_{0.15}\text{Au}_{0.25}\text{Pd}_{0.60}/\text{N-SiO}_2$ catalyst in the FA dehydrogenation (0.20 M in 10.0 mL H_2O) at 298 K.

10 ppm). In other words, these experiments point to the important fact that CO -free H_2 generation can be achieved in the absence of additives even at room temperature from an aqueous FA solution for fuel cell applications⁴ by utilizing a $\text{Cr}_{0.15}\text{Au}_{0.40}\text{Pd}_{0.60}/\text{N-SiO}_2$ catalyst. Fig. 2(d) shows the plot of the volume of generated gas ($\text{CO}_2 + \text{H}_2$) versus time for $\text{Cr}_{0.15}\text{Au}_{0.40}\text{Pd}_{0.60}/\text{N-SiO}_2$ catalyzed dehydrogenation of aqueous FA solution (0.20 M in 10.0 mL H_2O) at different catalyst concentrations ([CrAuPd]). We found that only 2.0 mol % of $\text{Cr}_{0.15}\text{Au}_{0.40}\text{Pd}_{0.60}/\text{N-SiO}_2$ can catalyze dehydrogenation of FA at complete conversion with an *initial* TOF value of 730 mol H_2 mol catalyst⁻¹ h⁻¹. To the best of our knowledge, this is the highest TOF value ever reported for FA dehydrogenation at room temperature using a heterogeneous catalyst without utilizing any additives (Table 1) and is even comparable to most homogeneous catalysts.⁶ More importantly; the dehydrogenation of FA can be completed within a 10 min. at > 99 % conversion measured at 298 K. The reaction rates for each catalyst concentration were calculated from the linear portion of each plot given in Fig. 2(d). The logarithmic plot of the hydrogen generation rate versus catalyst concentration (Fig. S7, ESI[†]) gives a line with a slope of 1.13 which indicates that $\text{Cr}_{0.15}\text{Au}_{0.40}\text{Pd}_{0.60}/\text{N-SiO}_2$ catalyzed additive-free FA dehydrogenation, is close to first-order with respect to the catalyst concentration within the investigated concentration window.

In addition to the catalyst concentration, we also investigated the effect of temperature on the rate of FA dehydrogenation by performing the catalytic reaction at different temperatures (Figure 2(f)). It is apparent that $\text{Cr}_{0.15}\text{Au}_{0.40}\text{Pd}_{0.60}/\text{N-SiO}_2$ catalyst works more effectively at elevated temperatures (> 298 K), the *initial* TOF values of 1280, 2030, 3360 and 4700 mol H_2 mol catalyst⁻¹ h⁻¹ at 308, 318,

328 and 338 K, respectively. The reaction rates for each catalyst concentration were calculated from the linear portion of each plot

Table 1. Comparison of the catalytic performance of CrAuPd/N-SiO₂ catalyst with the prior best heterogeneous catalyst systems reported for the dehydrogenation of FA in the absence of any additives at ≤ 298 K.

Catalyst	Temp.(K)	Con. (%)	Activity ^[a]	Reference
Ag@Pd	293	36	63	[8a]
AgPd	293	10	72	[8a]
Ag@Pd/C	293	44	96	[8a]
Au@Pd/N-rGO	298	89	98	[8b]
CoAuPd/C	298	91	37	[8c]
CoAuPd/r-GO	298	51	45	[8d]
CoAuPd/DNA	298	96	85	[8d]
AuPd	298	28	41	[8e]
AgPd	298	52	150	[8f]
Pd-MnO _x /N-SiO ₂	293	80	140	[8g]
CrAuPd/N-SiO ₂	298	100	730	this study

[a] *initial* TOF values (TOF = mol H_2 / mol catalyst × time (h)) calculated at ~ 20 % of conversion achieved.

The values of observed rate constants k_{obs} determined from the linear portions of the volume of generated gas ($\text{CO}_2 + \text{H}_2$) versus reaction time plots at five different temperatures are used to obtain Arrhenius and Eyring plots (Fig. S8 and S9, ESI[†]) to calculate activation parameters. Using these plots, apparent activation energy (E_a), apparent activation enthalpy (ΔH_a^\ddagger) and apparent activation entropy (ΔS_a^\ddagger) values were calculated to be 49.8 kJ/mol, 47.4 kJ/mol and -65.1 J/mol.K, respectively. Assuming that the apparent activation parameters calculated from the macroscopic

kinetic data given above are relevant to the most critical activation step in the FA dehydrogenation mechanism, one can argue that the small positive value apparent activation energy and the large negative value of apparent activation entropy imply the presence of associative mechanism in the transition state.¹⁴ Then, to understand the effect of surface grafted amine group on the catalytic reactivity of CrAuPd NPs, we conducted a control experiment, in which the activity of CrAuPd NPs supported on amine-free SiO₂ was investigated in the FA dehydrogenation under identical conditions. We found amine-free SiO₂ supported CrAuPd catalyst (Cr_{0.13}Au_{0.27}Pd_{0.60}/SiO₂) provides lower catalytic performance (TOF = 120 mol H₂ mol catalyst⁻¹ h⁻¹ and 42 % conversion) than that of Cr_{0.15}Au_{0.40}Pd_{0.60}/N-SiO₂ (Fig. S10, ESI[†]). The lower reactivity of Cr_{0.15}Au_{0.40}Pd_{0.60}/N-SiO₂ can be explained by the absence of -NH₂ functionalities on the support material, which may have a direct impact on the FA adsorption/storage process as well as the nucleation and growth of the CrAuPd NPs on the support surface. CTEM image of Cr_{0.13}Au_{0.27}Pd_{0.60}/SiO₂ catalyst (Fig. S11, ESI[†]) reveals that the existence of highly clumped particles with respect to Cr_{0.15}Au_{0.40}Pd_{0.60}/N-SiO₂, which shows the stabilizing effect of surface grafted amine groups.¹⁵ Additionally, Yamashita *et al.*¹⁶ reported that Pd or Ag@Pd NPs supported on a resin bearing -N(CH₃)₂ acted as more efficient organic support than those of bearing -SO₃H, -COOH and -OH in the catalytic decomposition of FA. According to the results of their detailed mechanistic studies, it was found that O-H bond cleavage is facilitated with the assistance of -N(CH₃)₂ group and leads to the formation of metal-formate species along with a -[N(CH₃)₂H]⁺ group, which, then, undergo further dehydrogenation to produce H₂ and CO₂. In the light of these results, it is reasonable to understand that the existence of surface grafted amine in our support acts as a proton scavenger and provides a basic environment around CrAuPd NPs, which benefits the O-H bond dissociation that is subsequently associated with the C-H bond cleavage from the metal-formate intermediate to release H₂.

The catalytic stability of the Cr_{0.15}Au_{0.40}Pd_{0.60}/N-SiO₂ catalyst was investigated by performing recycling and reusability experiments (Fig. 2(f)). When all of FA was converted to CO₂ and H₂ in a particular cycle, more FA was added into the solution and the reaction was continued up to five consecutive catalytic cycles. It was found that Cr_{0.15}Au_{0.40}Pd_{0.60}/N-SiO₂ catalyst shows high stability and retains 70 % of its initial activity and provides 95 % of conversion without CO generation after the 5th consecutive cycle. Isolability and reusability characteristics of Cr_{0.15}Au_{0.40}Pd_{0.60}/N-SiO₂ were also tested in the FA dehydrogenation under identical conditions. After the complete dehydrogenation of FA, catalyst was isolated as a dark gray powder and bottled under nitrogen atmosphere. Then, it was re-dispersed in the aqueous FA solution. This re-dispersed catalyst preserved 50 % of its initial activity with 80 % conversion of FA to CO₂ and H₂ even after the 5th catalytic reuse. CTEM analyses of recovered samples after 5th consecutive catalytic run of the recycling and reusability experiments (Figs. S12-S13, ESI[†]) show a slight increase in the average particle size of Cr_{0.15}Au_{0.40}Pd_{0.60}/N-SiO₂ (2.9 and 4.2 nm, respectively) consistent with the observed decrease in the activity at the end of these experiments. XPS spectrum of reused sample shows that there is no significant change in the chemical states of Pd, Au and Cr (Fig. S14,

ESI[†]). Moreover, ICP-OES and elemental analyses of recovered Cr_{0.15}Au_{0.40}Pd_{0.60}/N-SiO₂ catalyst samples and reaction solution indicated that metal and -NH₂ contents of the catalysts remained intact after recycle and reusability experiments. Additionally, removing the Cr_{0.15}Au_{0.40}Pd_{0.60}/N-SiO₂ catalyst from the reaction solution can completely stop the dehydrogenation of FA. These results are indicative of the high stability of CrAuPd NPs against leaching throughout the catalytic runs. In summary, amine grafted silica supported CrAuPd NPs have been reproducibly synthesized and preliminarily characterized by the combination of multi-pronged techniques. The resulting Cr_{0.15}Au_{0.40}Pd_{0.60}/N-SiO₂ catalyst revealed a record activity (730 mol H₂ mol catalyst⁻¹ h⁻¹) and excellent conversion (> 99 %) converging to that of the existing state of the art homogenous catalytic systems available for the room temperature dehydrogenation of FA in the absence of any additives. Understanding the existing synergistic effects of Cr_{0.15}Au_{0.40}Pd_{0.60}/N-SiO₂ catalyst remains an active area of research in our group. More detailed experimental studies on the mechanism of Cr_{0.15}Au_{0.40}Pd_{0.60}/N-SiO₂ catalyzed dehydrogenation of FA are still underway. This uniquely active, selective and stable catalytic material has a strong potential to be exploited in practical/technological applications, where FA is utilized as a viable hydrogen carrier in mobile fuel cell applications.

Notes and references

- L. Schlapbach, A. Züttel, *Nature*, 2001, **414**, 353.
- J. A. Turner, *Science*, 1999, **285**, 687.
- M. Yadav, Q. Xu, *Energy Environ. Sci.*, 2012, **5**, 9698.
- K.V. Kordesch, G.R. Simader, *Chem. Rev.*, 1995, **95**, 191.
- T.C. Johnson, D.J. Morris, M. Wills, *Chem. Soc. Rev.*, 2010, **39**, 81-88.
- A. Boddien, D. Mellmann, F. Gaertner, R. Jackstell, H. Junge, P. J. Dyson, G. Laurenczy, R. Ludwig, M. Beller, *Science*, 2011, **333**, 1733.
- A. Bulut, M. Yurderi, Y. Karatas, M. Zahmakiran, H. Kivrak, M. Gulcan, M. Kaya, *App. Catal B: Env.*, 2014, **160**, 514.
- (a) K. Tedsree, T. Li, S. Jones, C.W.A. Chan, K.M.K. Yu, P.A. Bagot, E.A. Marquis, G.D.W. Smith, S.C.E. Tsang, *Nat. Nanotech.*, 2011, **6**, 302; (b) Z. L. Wang, J.M. Yan, H.L. Wang, Y. Ping, Q. Jiang, *J. Mater. Chem. A*, 2013, **1**, 12721; (c) Z. L. Wang, J.M. Yan, Y. Ping, H.L. Wang, W.T. Zheng, Q. Jiang, *Angew. Chem. Int. Ed.*, 2013, **52**, 4406; (d) Z. L. Wang, H.L. Wang, J. M. Yan, Y. Ping, S. H. O, S. J. Li, Q. Jiang, *Chem. Commun.*, 2014, **50**, 2732; (e) Ö. Metin, X. Sun, S. Sun, *Nanoscale*, 2013, **5**, 910; (f) Zhang, Ö. Metin, D. Su, S. Sun, *Angew. Chem. Int. Ed.*, 2013, **52**, 3681; (g) A. Bulut, M. Yurderi, Y. Karatas, M. Zahmakiran, H. Kivrak, M. Gulcan, M. Kaya, *App. Catal B: Env.*, 2015, **164**, 324.
- See Electronic Supplementary Information (ESI) for details.
- I. Taylor, A. G. Howard, *Anal. Chim. Acta*, 1993, **271**, 77.
- J. He, Y. Zhang, E. Y.-X. Chen, *ChemSusChem*, 2013, **6**, 61.
- J. S. Yoo, F. A. Pedersen, J. K. Nørskov, F. Studt, *ACS Catal.*, 2014, **4**, 1226; J. A. Herron, J. Scaranto, P. Ferrin, S. Li, M. Mavrikakis, *ACS Catal.*, 2014, **4**, 4434.
- R. Ferrando, J. Jellinek, R. L. Johnston, *Chem. Rev.*, 2008, **108**, 845.
- K. A. Connors, *Theory of Chemical Kinetics*; VCH Publishers: New York, 1990.
- M. Zahmakiran, M. Tristany, K. Philippot, K. Fajerweg, S. Özkar, B. Chaudret, *Chem. Commun.*, 2010, **46**, 2938.
- K. Mori, M. Dojo, H. Yamashita, *ACS Catal.* 2013, **3**, 1114